JACS
JOURNAL OF THE AMERICAN CHEMICAL SOCIETY

COMMUNICATION

pubs.acs.org/JACS

Two-Photon Pumped Lasing in Single-Crystal Organic Nanowire Exciton Polariton Resonators

Chuang Zhang,[†] Chang-Ling Zou,[‡] Yongli Yan,[†] Rui Hao,[†] Fang-Wen Sun,[‡] Zheng-Fu Han,[‡] Yong Sheng Zhao,[*,†] and Jiannian Yao[*,†]

[†]Beijing National Laboratory for Molecular Sciences, Key Laboratory of Photochemistry, Institute of Chemistry, Chinese Academy of Sciences, Beijing 100190, China

[‡]Key Laboratory of Quantum Information, University of Science and Technology of China, Hefei, Anhui 230026, China

Supporting Information

ABSTRACT: Single-crystal organic nanowires were fabricated with a soft-template-assisted self-assembly method in liquid phase. These nanowires with rectangular cross section can serve as resonators for exciton−photon coupling, leading to a microcavity effect and a relatively low threshold of laser actions. Two-photon-pumped blue lasing was observed in these organic waveguiding nanostructures above a threshold of 60 nJ, excited with a 750 nm near-infrared femtosecond pulse laser at 77 K.

Organic dyes exhibiting two-photon pumped (TPP) lasing based on two-photon absorption (TPA) molecular structures have received increasing attention due to the broad range of possible applications in wavelength upconversion, 3D fluorescence imaging, and 3D microfabrication.[1] Unlike common second-harmonic generation in second-order nonlinear crystals, TPP lasing provides a possible way to accomplish frequency upconversion of coherent light within a broad spectral range but without phase-matching requirements.[2] However, traditional organic TPP lasers in liquids, films, solid rods, optical fibers, and artificial optical microcavites often require relatively high pump power due to the nonlinear nature of TPA. To create low-power TPP lasers, tiny devices, e.g., organic nanowire TPP lasers, are desired to minimize the energy required to transport the electrons to their upper states.[3] In addition, single-crystalline organic nanowires can be synthesized[4] and integrated[5] readily, which exhibit excellent performances of photon confinement and propagation[6] and high charge-carrier mobilities[7] for future electrically pumped laser devices.

The strong coupling between excitons and photons can result in the formation of exciton polaritons (EPs) in semiconductor microcavities,[8] which are mixed light-matter quasiparticles that combine the best features of photonics and excitonic systems.[9] In organic materials, excitons and EPs are highly stable because of their large binding energies, showing long-distance exciton migration and propagation of EPs in organic dye nanofibers.[10,11] Therefore, TPP lasers in organic crystalline nanowires may offer a low excitation threshold according to the stable existence of EPs confined in nanowire microcavities.[12] To our knowledge, the fabrication of single-crystalline 1D nanostructures from TPA molecules remains challenging because of their specific donor−π-bridge−acceptor structures.[13] Following our continuous investigations on intermolecular interactions and successful fabrication of 1D organic structures,[14] herein well-defined organic nanowires of TPA molecules are designed and synthesized with a surfactant-assisted self-assembly method. These nanostructures can work as efficient resonators for the strong exciton−photon coupling and are capable of emitting laser around 475 nm at low-power excitation according to our loss/gain calculation in the EP model. When a single wire was excited locally with a near-infrared pulse laser, blue TPP lasing was observed in the resonance modes of EPs above a threshold of 60 nJ. This low-threshold frequency-upconversion nanowire laser is expected to be integrated with the traditional downconversion elements to compose integral photonic circuits at nanoscale.[15]

In this work, 2-(*N*,*N*-diethylanilin-4-yl)-4,6-bis(3,5-dimethylpyrazol-1-yl)-1,3,5-triazine (DPBT, Figure 1) was designed and synthesized for its high quantum yield in two-photon excitation fluorescence[16] and preponderant molecular packing along the *c* crystal axis. Single-crystalline nanowires were prepared by injecting a tetrahydrofuran (THF) solution of DPBT into aqueous solutions of cetyltrimethylammonium bromide (CTAB) at different temperatures (see Supporting Information). As shown in the photoluminescence (PL) image in Figure 1A, the as-prepared DPBT nanostructures have uniform 1D wire-like morphology and emit strong blue PL with bright spots at the wire ends (see inset) under unfocused UV excitation. This characteristic of optical waveguiding indicates that PL energy can propagate efficiently along the axis direction, which is attributed to the smooth surface and defect-free structure of the nanowires, as shown in the scanning electron microscopy (SEM) image in Figure 1B. The flatness of the surface and the rectangular shape of cross section are clearly illustrated in the atomic force microscopy (AFM) image (Figure S1). The transmission electron microscopy (TEM) image and selected area electron diffraction (SAED) pattern in Figure 1C indicate that the wire is a single crystal growing along the [001] direction with flat end facets. The flat end facets can efficiently reflect the guided PL, which is essential for optical gain and amplification of stimulated emission.[17] Figure 1D displays the molecular packing in a DPBT crystal, revealing strong $\pi-\pi$ stacking and primary growth along the *c* crystal axis. The preferential

Received: January 19, 2011
Published: April 25, 2011

dx.doi.org/10.1021/ja200549v | *J. Am. Chem. Soc.* 2011, 133, 7276–7279

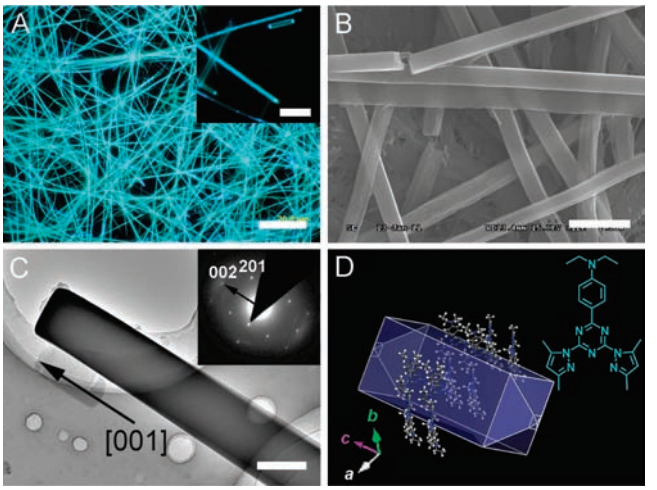

Figure 1. (A) PL image of the DPBT nanowires excited with the UV band (330−380 nm) light source; scale bar is 25 μm. Inset: magnified image of several wire ends; scale bar is 5 μm. (B) SEM image of the nanowires with uniform diameter and smooth surfaces; scale bar is 2 μm. (C) TEM image of a single DPBT wire; scale bar is 500 nm. Inset: SAED pattern of the wire. (D) Theoretically predicted growth morphology of a single crystal of DPBT. Inset: molecular structure.

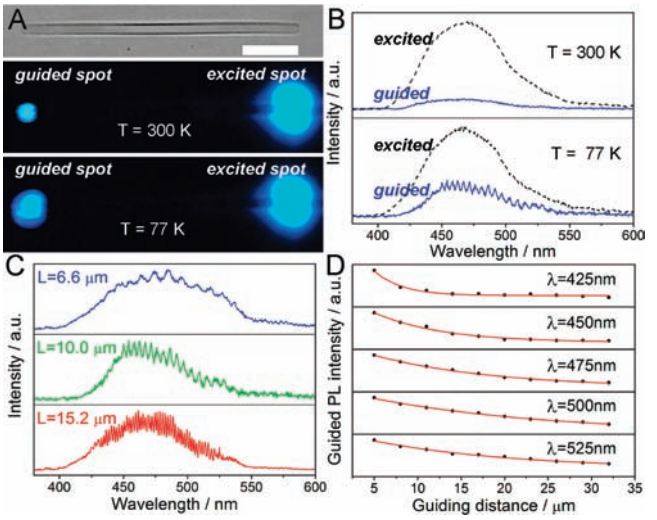

Figure 2. (A) Bright-field microscopy image and PL images of a single DPBT nanowire taken at room temperature (300 K) and liquid nitrogen temperature (77 K), respectively; scale bar is 2 μm. (B) Corresponding PL spectra of the excited spots (black dashed lines) and guided spots (blue lines) in the PL images in (A). (C) Modulated PL spectra collected at guided tips of three DPBT nanowires with different lengths. (D) Decay of the guided PL intensity at different wavelengths as an exponential function of the propagation distance.

growth along the [001] direction can be induced by the CTAB micelles, which leads to the formation of 1D nanostructures.[18] The excellent crystallinity can further improve the exciton−photon coupling and the migration of excitons in the light guiding process.

The TPA cross section of DPBT is as large as 160 GM (1 Göppert-Mayer unit, 1 GM = 10^{-50} cm^4 s photon^{-1} molecule^{-1}) around 750 nm (Figure S2), so a focused 750 nm femtosecond pulse laser was adopted to locally excite the two-photon fluorescence of the DPBT nanowires. Figure 2A shows the light guiding of two-photon excited PL signals from the excited right wire tip to the left tip, which indicates that the energy of EPs can propagate along the wire axis and outcouple as PL photons at tips. Interestingly, the guided PL spot at 77 K is much brighter than that at 300 K, although the excitation intensity and guiding distance are kept constant. This enhanced guided PL at low temperature was more accurately determined with the emission spectra as shown in Figure 2B, which reveals that the optical loss in the guiding process at 77 K is only half of that at 300 K. More importantly, the significant decrease in optical loss at 77 K induces a series of PL modulations formed from Fabry−Pérot (FP) modes between the two end facets. The re-absorption loss in light guiding from the overlaps between emission and absorption can be significantly reduced in EP coupling because of the increased stability of excitons at low temperature. In organic materials, the stability of Frenkel excitons and the coupling between excitons and photons is determined by the exciton binding energy.[11,19] The thermal disturbance at liquid nitrogen temperature is $kT_{77K} \approx 7.7$ meV, which is much lower than that at room temperature ($kT_{300K} \approx 30$ meV). Accordingly, Frenkel excitons become stable enough at 77 K to form EPs with photons that can travel back and forth along the crystalline wire axis coherently, which may help in the FP-type resonance in the 1D nanostructure.

The PL spectra of the outcoupling light at 77 K from the tips in DPBT nanowires with different lengths (L = 6.6, 10.0, 15.2 μm) were measured to study the relationship between the FP-type resonance modes and the size of the nanowire microcavity. As shown in Figure 2C, the modulated PL spectra of the outcoupled emission present an increasing number of FP modes with increasing cavity length in the EP resonators. For the PL spectra of FP-type resonance, the mode spacing is given by $\Delta\lambda = \lambda^2/2Ln_g$, where L is the length of the nanowire resonator, λ is the light wavelength, and n_g is the group refractive index as a function of the wavelength.[20] The modes emerge at the lower energy side but do not appear at shorter wavelengths because the exciton character of the EPs changes through coupling with acoustic phonons. During the propagation of EPs, continuous absorption and re-emission of PL occurs, leading to the guided distance-dependent PL intensities at different wavelengths (Figure S3). As shown in Figure 2D, the PL intensity decays exponentially at shorter wavelengths but much more slowly at longer wavelengths as a function of propagation distance. The nearly linear decay at longer wavelengths can be attributed to the weaker absorption of lower energy EPs and continuous re-emission in EP propagation.[6] These results indicate that a lower propagation loss is expected at longer wavelengths within the emission range in these EP resonators.

To verify the existence of EP resonance in the obtained nanowires, we calculated the accurate complex refractive index of DPBT crystals in the propagation direction of [001] from the obtained PL data. First, the group refractive index n_g along the axis is calculated from $n_g = \lambda^2/2L\Delta\lambda$ by measuring the peak spaces $\Delta\lambda$ in modulated PL spectra in Figure 2C. Plots of n_g versus λ for the three lengths are shown in Figure 3A, which indicates that n_g is about 2.1 at longer wavelength in the emission band and suddenly increases at shorter wavelength. The PL intensity at guided spots is then given by $I = I_0 \exp[-2\omega \mathrm{Im}(n)X/c]$, where I_0 is the PL intensity at the excited spot, ω is the frequency of the light, $\mathrm{Im}(n)$ is the imaginary part of the refractive index, X is the propagation distance, and c is the speed of light. The $\mathrm{Im}(n)-\lambda$ relationship can be plotted as shown in Figure 3B from

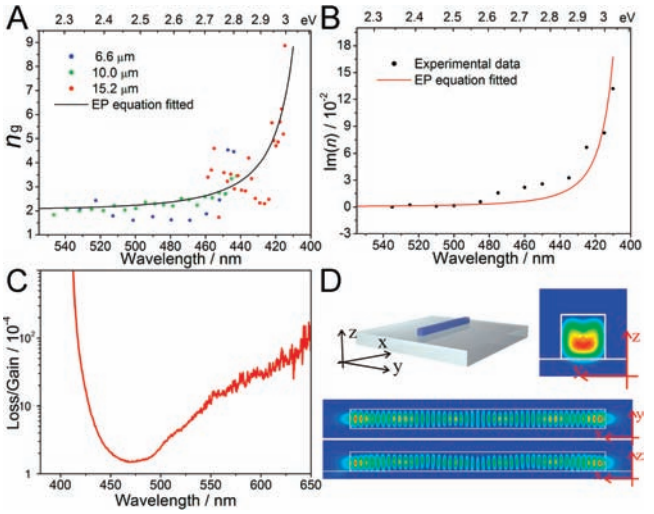

Figure 3. (A) Group refractive index n_g and (B) imaginary part of the complex refractive index Im(n) versus wavelength along the [001] direction in single-crystalline DPBT nanowires at 77 K. The fitted curves are calculated according to the EP model in optical waveguiding. (C) Simulated loss/gain versus wavelength in the 6.6 μm long DPBT nanowire at 77 K. (D) Simulated electric field intensity distribution (λ = 475 nm, n = 1.767) in the DPBT nanowire at 77 K which is 6.6 μm long, 500 nm wide, and 500 nm high.

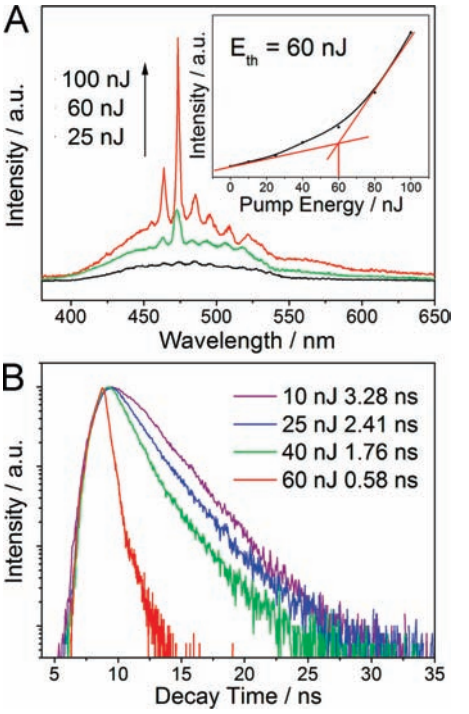

Figure 4. (A) PL spectra recorded at the tip of the 6.6 μm long DPBT nanowire excited at different energies (25, 60, and 100 nJ) at 77 K. Inset: power dependence profile of PL intensities at the tip of the same nanowire. (B) PL decay profiles of the same nanowire excited at different energies (10, 25, 40, and 60 nJ) at 77 K. The PL lifetime shows a sharp decrease at 60 nJ pump energy.

the optical loss versus propagation distance in Figure 2D. The Im(n) shows a dependence on PL wavelength identical to that of n, especially when the photon energy is larger than 2.7 eV. The complex refractive index shows strong dispersion in high photon energy bands, which is characteristic of EP from the strong coupling between excitons and photons.[21] The dispersion curve shows distinguishing features of propagation of EP in 1D organic nanostructures, very different from those of either uncoupled light or exciton. This result confirms that the formed EP may cause resonance and amplification of the PL emission in these single-crystalline nanowires.

The optical loss and gain in the nanowire EP resonators are calculated to study the possibility of optically pumped TPP lasing. It is well known that the laser action is possible only when the optical gain is larger than the optical loss. Three major factors were taken into account in the determination of the loss/gain ratios of different FP modes: the outcoupling and reflection at the end facets, the optical gain of the dye DPBT, and the absorption loss in the guiding process. The reflectivity at the end facets can be evaluated from the Fresnel equation with normal incidence $R = ((n-1)/(n+1))^2$, where n is the phase refractive index (see Supporting Information), and the corresponding reflection loss can be estimated as $\gamma = -(\ln R)/L$.[22] The gain is determined by the spatial spectra and the spectral overlap between the resonance and the gain material. The absorption loss as light travels is derived directly from the decay of the guided PL intensity at different wavelengths in Figure 2D. In this work, the scale of the nanowire waveguide is nearly the same as the PL wavelength, so almost all the radiative energy can be confined in the nanowire microcavity. In our numerical simulation, the overlap of the cavity mode with the gain medium is >95% and insensitive to the wavelength in the range of 380−650 nm. Considering all these factors, we estimate the loss/gain curve versus PL wavelength in Figure 3C, which illustrates the possibilities of lasing action over the emission spectra range. A minimum value is noted in the loss/gain curve at ~475 nm, which theoretically predicts that the FP modes nearby might be pumped at relatively low threshold energies.

The properties of the FP resonance in the nanowire are investigated with the three-dimensional finite element method. The electric field intensity at 475 nm (n = 1.767) in the selected single wire (6.6 μm long, 500 nm wide, and 500 nm high) on a silica substrate (n = 1.45) is described in Figure 3D. The electric field intensity at the cross section reveals that the energy of the electric field is well confined in the nanostructures as EP resonators, and the scattering into the air and the substrate is quite limited. The mode profiles along the nanowire clearly show the efficient light guiding, along with the reflection and leak-out at the end facets, which indicate a typical FP-type EP resonance. Here we do not consider the transverse magnetic polarization modes, as they are poorly confined and reflected at the end facets in the nanowires. According to the calculation of the possible laser action in the EP resonators, the pump power was increased to locally excite the 6.6 μm long DPBT nanowire. As displayed in Figure 4A, PL peaks in the spectra strongly depend on the increase of pump energy of the pulse laser (λ = 750 nm, ~200 fs). At a low excitation power of 25 nJ, the PL spectrum displays broad FP modes over the entire emission band, almost the same as the spectra in Figure 2C. However, a sharp cavity mode at 475 nm above the onset power as an amplified spontaneous emission was observed at excitation power of 60 nJ. At a higher excitation power of 100 nJ, the full-width at half-maximum (fwhm) at 475 nm narrows to 2.9 nm, and the sharp peaks at ~465 and 485 nm can also be clearly observed, which justifies the calculated curve of laser action in Figure 3C.

The inset in Figure 4A illustrates the energy dependence of PL intensity, showing an obvious energy threshold at ~60 nJ,

dx.doi.org/10.1021/ja200549v | J. Am. Chem. Soc. 2011, 133, 7276–7279

which reveals a nonlinear gain and a threshold characteristic of a laser. To verify the TPP laser action above the threshold, we measured the PL decay profiles at different pump energies, which indicate that the PL lifetime gradually decreases as the pumped power increases (below the threshold) and sharply falls to 0.58 ns at 60 nJ (above the threshold), as shown in Figure 4B. These results demonstrate that the resonance of EPs not only plays an important role in light propagation but also leads to the interference and enhancement of PL emission in the nanowires as miniaturized optical microcavties. The quality factor Q in this microcavity is as high as 57.0, attributed to the optically flat surface and the existence of EPs, which agrees well with the estimation from end facet reflectivity, $Q = 2n\pi/\lambda\gamma = 60.1$. The nanowires show great potential in fabricating laser devices, considering its relatively high Q-factor among organic nanostructures. The significant spectral line narrowing (fwhm = 2.9 nm), the existence of laser cavity resonances, the clear indication of a threshold (E_{th} = 60 nJ), and the short emission lifetime above threshold (τ = 0.58 ns) verify the TPP lasing in this kind of organic single-crystalline nanowire EP resonators.

Organic nanowires, as typical optical waveguiding structures, can lead to FP-type PL modulation and some properties of laser light because waveguides are common laser geometry.[23] The interaction between photons and excitons is determined by the ratio of the oscillator strength to the mode volume. Therefore, it is the very high oscillator strength of the Frenkel excitons rather than any cavity effect that causes EPs to exist in the presented DPBT nanowires. Although the distinctions between polariton-type and photon-type lasing remain subtle in organic nanostructures,[24,25] the existence of EPs should play an essential role in optical waveguiding and TPP lasing according to our experiments. In agreement with calculation from the EP model in selected DPBT nanowires, the strong dispersion and resonance of EP leads to an efficient optical gain around 475 nm in the microcavity. In our experiments, TPP lasing in the EP resonators can only be pumped at low temperature. However, this kind of model TPP nanolaser device based on EP effects in organic waveguides might provide enlightenment for other organic EP devices and find application in miniaturized photonics integrations.

In conclusion, single-crystalline nanowires were prepared from an organic TPA compound, DPBT, via surfactant-assisted self-assembly in aqueous solution. These nanowires can serve as EP resonators at 77 K because of the increased stability of the strong coupling between photons and Frenkel excitons. Single-nanowire TPP lasing was observed around 475 nm, pumped with a 750 nm pulse laser above a threshold of 60 nJ. The low driving power can be attributed to the EP resonance in the nanowire microcavity. The Q factor in this microcavity is as high as 57.0 because of the optically flat surfaces and the existence of EPs in the nanostructures. This approach to organic crystalline TPP nanolasers in 1D organic nanostructures may lead to a new series of upconverted organic photonic devices.[26]

■ ASSOCIATED CONTENT

Supporting Information. Experimental details; optical characterization; discussion on EP model; AFM image and cross section profile; TPA cross section of DPBT; and spatially resolved spectra at the wire tip. This material is available free of charge via the Internet at http://pubs.acs.org.

■ AUTHOR INFORMATION

Corresponding Author
yszhao@iccas.ac.cn; jnyao@iccas.ac.cn

■ ACKNOWLEDGMENT

This work was supported by National Natural Science Foundation of China (Nos. 51073164, 91022022), the Chinese Academy of Sciences, and the National Basic Research 973 Program of China.

■ REFERENCES

(1) He, G. S.; Tan, L. S.; Zheng, Q.; Prasad, P. N. *Chem. Rev.* **2008**, *108*, 1245–1330.
(2) Reinhardt, B. A.; Brott, L. L.; Clarson, S. J.; Dillard, A. G.; Bhatt, J. C.; Kannan, R.; Yuan, L. X.; He, G. S.; Prasad, P. N. *Chem. Mater.* **1998**, *10*, 1863–1874.
(3) O'Carroll, D.; Lieberwirth, I.; Redmond, G. *Nat. Nanotechnol.* **2007**, *2*, 180–184.
(4) Zhao, Y. S.; Fu, H. B.; Peng, A. D.; Ma, Y.; Xiao, D. B.; Yao, J. N. *Adv. Mater.* **2008**, *20*, 2859–2876.
(5) Zhao, Y. S.; Wu, J. S.; Huang, J. X. *J. Am. Chem. Soc.* **2009**, *131*, 3158–3159.
(6) Takazawa, K.; Kitahama, Y.; Kimura, Y.; Kido, G. *Nano Lett.* **2005**, *5*, 1293–1296.
(7) Jiang, L.; Fu, Y. Y.; Li, H. X.; Hu, W. P. *J. Am. Chem. Soc.* **2008**, *130*, 3937–3941.
(8) Hopfield, J. J.; Thomas, D. G. *Phys. Rev. Lett.* **1965**, *15*, 22–25.
(9) Andreani, L. C.; Panzarini, G.; Gerard, J. M. *Phys. Rev. B* **1999**, *60*, 13276–13279.
(10) Chaudhuri, D.; Li, D.; Che, Y.; Shafran, E.; Gerton, J. M.; Zang, L.; Lupton, J. M. *Nano Lett.* **2011**, *11*, 488–492.
(11) Takazawa, K.; Inoue, J.; Mitsuishi, K.; Takamasu, T. *Phys. Rev. Lett.* **2010**, *105*, 067401.
(12) van Vugt, L. K.; Ruhle, S.; Ravindran, P.; Gerritsen, H. C.; Kuipers, L.; Vanmaekelbergh, D. *Phys. Rev. Lett.* **2006**, *97*, 147401.
(13) Gao, F.; Liao, Q.; Xu, Z. Z.; Yue, Y. H.; Wang, Q.; Zhang, H. L.; Fu, H. B. *Angew. Chem., Int. Ed.* **2010**, *49*, 732–735.
(14) Zhao, Y. S.; Fu, H. B.; Peng, A. D.; Ma, Y.; Liao, Q.; Yao, J. N. *Acc. Chem. Res.* **2010**, *43*, 409–418.
(15) Yan, R. X.; Gargas, D.; Yang, P. D. *Nat. Photon.* **2009**, *3*, 569–576.
(16) Fu, L. M.; Wen, X. F.; Ai, X. C.; Sun, Y.; Wu, Y. S.; Zhang, J. P.; Wang, Y. *Angew. Chem., Int. Ed.* **2005**, *44*, 747–750.
(17) Yan, H. Q.; Johnson, J.; Law, M.; He, R. R.; Knutsen, K.; McKinney, J. R.; Pham, J.; Saykally, R.; Yang, P. D. *Adv. Mater.* **2003**, *15*, 1907–1911.
(18) Lei, Y. L.; Liao, Q.; Fu, H. B.; Yao, J. N. *J. Am. Chem. Soc.* **2010**, *132*, 1742–1743.
(19) Scholes, G. D.; Rumbles, G. *Nat. Mater.* **2006**, *5*, 683–696.
(20) Sirbuly, D. J.; Law, M.; Yan, H. Q.; Yang, P. D. *J. Phys. Chem. B* **2005**, *109*, 15190–15213.
(21) van Vugt, L. K.; Piccione, B.; Agarwala, R. *Appl. Phys. Lett.* **2010**, *97*, 061115.
(22) Maslova, A. V.; Ning, C. Z. *Appl. Phys. Lett.* **2003**, *83*, 1237–1239.
(23) van Vugt, L. K.; Ru1hle, S.; Vanmaekelbergh, D. *Nano Lett.* **2006**, *6*, 2707–2711.
(24) Deng, H.; Weihs, G.; Santori, C.; Bloch, J.; Yamamoto, Y. *Science* **2002**, *298*, 199–202.
(25) Zhao, Y. S.; Peng, A. D.; Fu, H. B.; Ma, Y.; Yao, J. N. *Adv. Mater.* **2008**, *20*, 1661–1665.
(26) Zhang, C.; Zheng, J. Y.; Zhao, Y. S.; Yao, J. N. *Adv. Mater.* **2011**, *23*, 1380–1384.